Computers & Industrial Engineering 183 (2023) 109448

Contents lists available at ScienceDirect

Computers & Industrial Engineering

journal homepage: www.elsevier.com/locate/caie

Timetable optimization for maximization of regenerative braking energy utilization in traction network of urban rail transit ☆

Pengfei Sun [a], Chuanxin Zhang [a,b,*], Bo Jin [a,c], Qingyuan Wang [a], Haoran Geng [a,d]

[a] School of Electrical Engineering, Southwest Jiaotong University, Chengdu 611756, China
[b] POWERCHINA Jiangxi Electric Power Engineering Co.,LTD, Nanchang 330096, China
[c] Zhejiang Scientific Research Institute of Transport, Hangzhou 311305, China
[d] Green Science and Engineering Division, Sophia University, Japan

ARTICLE INFO

Keywords:
Urban rail transit
Traction network
Timetable optimization
Mixed integer quadratic programming
The overlap current method

ABSTRACT

Timetable optimization is one of the effective solution methods for urban rail transit to achieve energy-saving. Previous studies on timetable optimization only focused on the transfer and utilization of mechanical energy, which did not consider the exchange of energy and line losses in the traction network. Therefore, this paper constructs a cross-substation energy transmission and utilization model taking into account the characteristics of the actual traction power supply systems. An overlap current method is presented to increase the utilization of regenerative braking energy (RBE) of trains and reduce the energy supply of the traction substation by considering the line loss, which is achieved by compensating the current generated by accelerating and braking trains in the substation. The compensation current can be maximized by adjusting the dwell time to achieve energy-saving. The traction power supply systems with highly nonlinear dynamic characteristics are linearized to construct a mixed-integer linear programming (MILP) model, which utilizes the utilization of RBE as the objection and dwell time as the variable. The method of maximum compensation current is verified by numerical examples based on Beijing Batong Line. The results show that the energy-efficient of the method is greatly improved compared with the method of maximizing the overlap time between the accelerating train and the braking train.

1. Introduction

Urban rail transit has become a popular means of public transportation due to its large capacity, low energy consumption, safety, and punctuality (Zhang, Li, & Yang, 2019). However, the large-scale development of urban rail transit systems has also caused huge energy consumption. Climate change and energy are prominent global challenges. The implementation of energy-saving technologies has become particularly significant (Lin & Xie, 2014). Therefore, it is very necessary to carry out research on energy saving technology of urban rail transit. Regenerative braking is an energy recovery mechanism that has been widely utilized in rail transit systems around the world (Yang, Ning, Li, & Tang, 2014). Current research on the utilization and management of RBE can be divided into two categories (Liu, Zhou et al., 2018). The first category is to transfers the RBE generated by the braking train to the accelerating train for traction, and the maximum utilization of RBE can be achieved by optimizing the timetable, which is one efficient method that RBE is exploited in time. The second category is to utilize energy storage devices to store additional RBE, including onboard energy storage devices and trackside energy storage devices (Liu, Yang et al., 2018). On-board energy storage devices can avoid network losses to the greatest extent, but are subject to strict volume and weight restrictions, such as onboard supercapacitors (Zhong, Yang, Fang, Lin, & Tian, 2020), flywheels (Rupp, Baier, Mertiny, & Secanell, 2016), and batteries (Campillo, Ghaviha, Zimmerman, & Dahlquist, 2015). Although the ground energy storage technology is not limited by volume and weight, it has the problem of large network loss, including reversible power substations (Du et al., 2022; Pugi, Grasso, & Rossi, 2018), ground-based supercapacitors (Gao et al., 2015), etc. The existing systems cannot be fully upgraded and requires a large number of energy storage devices. Therefore, this paper mainly focuses on the first category of method, which helps to provide favorable conditions for the development of the second category of energy storage technology. Timetable optimization is currently the priority measure for improving the utilization efficiency of RBE in most urban rail transit systems in the world (González-Gil,

☆ This work was supported by the National Natural Science Foundation of China (Nos. U1934221, 62003283).
* Corresponding author at: School of Electrical Engineering, Southwest Jiaotong University, Chengdu 611756, China.
E-mail address: chuanxin0216@163.com (C. Zhang).

https://doi.org/10.1016/j.cie.2023.109448
Received 19 July 2022; Received in revised form 10 July 2023; Accepted 12 July 2023
Available online 28 July 2023

Palacin, & Batty, 2013). Timetable optimization is mainly to maximize the utilization of RBE and achieve energy-saving by adjusting the dwell time, departure interval, and running time of the train (Yang, Li, Gao, Wang, & Tang, 2012). Timetable optimization is a simple and efficient method. In practice, the urban rail transit systems adopt DC traction power supply systems (Yang, Chen, Li, Ning, & Tang, 2015). Due to the complexity of the system, timetable optimization focuses more on the transfer and utilization of mechanical energy, which did not consider the exchange of energy and line losses in the traction network. Therefore, the relevant research on timetable optimization based on traction network is carried out to further improve the energy efficiency of urban rail transit.

Urban rail transit has the characteristics of short departure intervals, large volumes, and frequent traction and braking, which will generate a large amount of RBE (Liu, Zhu, Bi, Liu and Xu, 2020). Part of the RBE generated by braking trains is utilized for onboard auxiliary systems, while most of the RBE will be fed back to the traction power supply systems. The accelerating train can utilize 60% of RBE generated by braking the train (Su, Wang, Cao, & Yin, 2019). The remaining RBE is mainly consumed on the grid in the form of heat through thermistors. It is very promising to improve the utilization of RBE and reduce energy consumption by optimizing the train timetable. Therefore, this paper has carried out the optimization of the energy-saving timetable considering the whole line of traction power supply systems.

Train timetables are the backbone of urban rail transit planning (Lindner, 2003). In 1971, Amit and Goldfarb first carried out research on train timetable optimization (Amit & Goldfarb, 1971). The quality of the timetable is closely related to the transportation requirements of the urban rail transit systems (Cordone & Redaelli, 2011). The current research on timetable optimization mainly includes several aspects (Huang, Yang, Tang, Cao, & Gao, 2016). Energy-saving studies aim to reduce the cost of the transportation sector (Li & Lo, 2014; Lindner, 2003). Stability studies aim to improve the robustness and reliability of train schedules (Liu, Schmidt et al., 2020; Meng & Zhou, 2011). Service quality studies aim to meet the demand of passenger flow and improve passenger comfort (Huang et al., 2016; Xie, Zhang, Sun, Ni, & Chen, 2021). There are also many studies on the restoration of timetables after disturbances (D'Ariano, Pranzo, & Hansen, 2007; Hong et al., 2021). The energy-saving timetable optimization is the most active among many types of research. The following mainly analyzes the previous research on energy-saving timetable optimization from the following aspects such as coordinated operation, DC traction power supply systems, optimization algorithm.

At present, the research on RBE utilization between trains has different problem assumptions and corresponding modeling descriptions. The main difference is how RBE can be exchanged or utilized. Taking the overlap time method as an example, different overlap locations have different impacts on the result. Coordinated trains in some stations include trains in adjacent station (Ramos, Pena, Fernández, & Cucala, 2008), trains in the same substation (Gupta, Tobin, & Pavel, 2016; Kim, Kim, & Han, 2011; Ning, Zhou, Long, & Tao, 2018; Pan, Chen, Lu, Tian, & Liu, 2020; Peña-Alcaraz, Fernández, Cucala, Ramos, & Pecharromán, 2012; Yin, Tang, Yang, Gao, & Ran, 2016), adjacent trains (Jin, Feng, Wang, Sun, & Fang, 2021), trains in the opposite direction in the same substation (Tang, Dick, & Feng, 2015; Xun, Liu, Ning, & Liu, 2019; Yang et al., 2012), trains in the same direction in the same substation (Yang et al., 2014), and so on. These studies ignore or simplify the power supply network to ensure that their problem is solvable, but in this way, it is ignored the influence of energy utilization between other substations. Although there are also some studies on coordinating trains in any substations to achieve global optimization (Lesel, Bourdon, Claisse, Debay, & Robyns, 2017; Li & Lo, 2014), but there is no effect or energy exchange between substations. In the bilateral power supply systems, all substations are interconnected, and the RBE generated by braking trains in any substations can be utilized by accelerating trains in any other stations. Due to the complexity of the system, there is currently no research to characterize the actual transfer and utilization of RBE between trains from a bilateral power supply system. Therefore, this paper constructs a cross-substation energy transmission and utilization model taking into account the characteristics of the actual traction power supply systems.

The energy consumption calculation method utilized in previous studies is the superposition of traction and braking energy in the same substation, but this method does not consider the efficiency and line losses of the traction power supply system. The theoretical results of these idealized energy transfer and exchange methods are quite different from the actual results, which seriously limited their application potential. Considering the DC traction power supply systems can more accurately represent the transfer and utilization of energy between trains. However, the power flow calculation method considering the traction power supply system has the problem of "state explodes" and "nonconvex problem". Few papers consider the influence of DC traction power supply systems in the research of timetable optimization. The utilization of Simulink simulation proved that timetable optimization considering DC the traction power supply systems can achieve energy-saving (Nasri, Moghadam, & Mokhtari, 2010). There are also papers that proposed a DC grid modeling technology to optimize the speed curve of a single train, which reduces the energy consumption of the substation (Tian et al., 2014). The DC traction power supply systems has the characteristics of a large-scale solution. Therefore, some studies often utilize distance-related energy-saving coefficients, while other studies only utilize the DC traction power supply systems model in the calculation of the results and do not utilize this model in the optimization process (Lesel et al., 2017; Peña-Alcaraz et al., 2012; Tang et al., 2015). Pan et al. proposed the unilateral AC power supply systems model for the first time and utilized a hybrid GA-PSO algorithm to timetable optimization (Pan et al., 2020). There are also some studies on the energy transfer and utilization between trains in unilateral power supply systems (Chen et al., 2019; Xiao, Feng, Wang, & Sun, 2020). The power supply network model established by these studies is often only modeled at a transient moment or an incomplete representation of the dynamic characteristics of the power supply systems, and the solution is extremely complicated. A method of maximum compensation current was proposed to ensure the effective utilization of RBE, which takes into account the exchange of energy and line losses in the traction network.

The MILP model has the characteristics of less restriction, easy promotion, and easy application, which is also a convenient online adjustment method. Ramos et al. first established a MILP model to maximize the overlap time of the acceleration train and the braking train (Ramos et al., 2008). MILP is a significant characteristic in timetable optimization, which is often utilized in many previous studies (Gupta et al., 2016; Jin, Feng, Wang, & Sun, 2022; Kim et al., 2011; Peña-Alcaraz et al., 2012; Shao, Xu, Sun, Kong, & Lu, 2022; Yang et al., 2019). These papers utilized only an energy-related indirect indicator to linearize the utilize of energy. There are also many papers that have established more direct energy index models and used heuristic algorithms to solve them. The most common heuristic algorithm in timetable optimization is to utilize a GA or a hybrid algorithm related to a GA (Lesel et al., 2017; Li & Lo, 2014; Liao, Zhang, Zhang, Yang, & Gong, 2021; Pan et al., 2020; Tang et al., 2015; Yang et al., 2012, 2014; Zhao et al., 2017). There are also algorithms such as artificial bee colony algorithm (Chen, Zuo, Lang, Li, & Li, 2022; Liu, Zhou et al., 2018), simulated annealing algorithm (Su et al., 2019), co-evolutionary algorithm (Bai et al., 2019), particle swarm algorithm (Meng, Jia, & Qin, 2010), dynamic programming algorithm (DP) (Yin et al., 2016), to solve the nonlinear problem in timetable optimization. Although the classical optimization method (the overlap time) based on MILP is widely utilized in the research of timetable optimization, the lack of consideration of the actual power supply network makes the energy-saving effect very limited. Therefore, a MILP model with the objective of maximizing the utilization of RBE was constructed for timetable

optimization, which linearizes the nonlinear traction power supply system and reduces the energy supply of the traction substation.

Most previous studies neither coordinate the trains between any substations to achieve global optimization nor consider adding a traction power supply systems to the optimization model. The traction power supply systems are linearized to construct a MILP with the utilization of RBE as the objection and dwell time as the variable in this paper. In order to achieve more accurate and practical modeling, the main contributions of this paper are as follows:

- For bilateral power supply systems, this paper constructs a cross-substation energy transmission and utilization model taking into account the characteristics of the actual traction power supply systems.
- A method of maximum compensation current was proposed to ensure the effective utilization of RBE, which takes into account the exchange of energy and line losses in the traction network. Meanwhile, the overlap current method with the same scale as the overlap time method is more practical in the traction power supply systems.
- A MILP model with the objective of maximizing the utilization of RBE was constructed for timetable optimization, which linearizes the nonlinear traction power supply system and reduces the energy supply of the traction substation.
- In the case studies, the iterative power flow calculation model of the DC traction power supply systems was utilized to demonstrate the energy-efficient of the method proposed in this paper.

The remainder of this paper is organized as follows. Section 2 defines the parameters and variables to better understand this paper. Section 3 constructs the constraint set of the timetable and presents the traditional overlap time method in timetable optimization. Section 4 is mainly to model and solution the DC traction network. Section 5 proposes the overlap current method and constructs an energy-saving schedule optimization model. Section 6 conducts a case study based on the Beijing Batong Line. Section 7 conclusions are presents.

2. Problem description

This paper discusses urban rail transit systems with J stations, N substations and a total of K trains pass through the systems in an orderly manner. In order to better understand this paper, a brief description of notations and decision variables is as follows:

2.0.1. Parameters

i, i'	Index of trains, $1 \le i, i' \le K$
j, j'	Index of stations, $1 \le j, j' \le J$
n	Index of substations, $1 \le n \le N$
$d_{j,min}$	Minimal dwell time at station j, (s)
$d_{j,max}$	Maximal dwell time at station j, (s)
$t_{j,j+1}$	Running time of train from station j to station $j+1$, (s)
t_{safe}	Minimal safe headway, (s)
$t_{a,j}$	Duration of the maximum accelerating phase from station j to station $j+1$, (s)
$t_{b,j}$	Duration of the maximum braking phase from station j to station $j+1$, (s)
$t^{min}_{i,i+1}$	Minimal headway time between train i and train $i+1$, (s)
$t^{max}_{i,i+1}$	Maximal headway time between train i and train $i+1$, (s)
$I(n,t)$	Current of substation n at time t, (A)
$P(n,t)$	Power of substation n at time t, (W)
$P_i(t)$	Power of train i at time t, (W)
$U_i(t)$	Voltage of train i at time t, (V)
$I_i(t)$	Current of train i at time t, (A)
U_s, R_s	Equivalent voltage and resistance of substation, (V, Ω)
$I_{in'}(n,t)$	Current generated in the substation n when the equivalent voltage source U_s of the substation n' and the equivalent current source $I_i(t)$ of the train i are acting separately, $1 \le in' \le K+N$, (A)
$U_{in'}(i,t)$	Voltage generated in the train i when the equivalent voltage source U_s of the substation n' and the equivalent current source $I_i(t)$ of the train i are acting separately, $1 \le in' \le K+N$, (V)

2.0.2. Variables

$t^{ov}_{i,j,i',j'}$	The overlap time between the maximum acceleration part of train i at station j and the maximum braking part of train i' at station j', (s)
$E_{i,j,i',j'}$	The RBE utilization when the maximum accelerating part of train i at station j overlaps the maximum braking part of train i' at station j', (kWh)
$\alpha_{i,j,i',j'}$	Logical variables related to whether the maximum accelerating part train i at station j and the maximum braking part overlap i' at station j'
$d_{i,j}$	Arrival time of train i at station j, (s)
$a_{i,j}$	Departure time of train i at station i, (s)

3. The classical optimization method—The overlap time

This section constructs the constraint set of the timetable. The timetable optimization model often uses the MILP model with logical variables. The MILP was applied to construct a model that maximizes the overlap time between the accelerating train and the braking train.

3.1. Modeling the constraint set

In order to generate a timetable that can meet the actual operation of trains, the following constraints are set:

(1) Headway Constraints: The departure interval of adjacent trains is often related to the quality of passenger transport services in urban rail transit. The Minimal headway of train i and train $i+1$ must be kept between $[t^{min}_{i,i+1}, t^{max}_{i,i+1}]$. The headway constraint at station j can be described as:

$$t^{min}_{i,i+1} \le d_{i+1,j} - d_{i,j} \le t^{max}_{i,i+1}, \quad \forall\, 1 \le i \le K-1, 1 \le j \le J \tag{1}$$

(2) Dwell Time Constraints: The dwell time of train i at station j is between $[d_{j,min}, d_{j,max}]$, and this range often depends on the passenger flow of the station. So the dwell time restriction can be described as:

$$d_{j,min} \le a_{i,j} - d_{i,j} \le d_{j,max}, \quad \forall\, 1 \le i \le K, \quad 1 \le j \le J-1 \tag{2}$$

(3) Safety Constraints: If the minimum safe headway of the train is set too small, it may cause a safety accident. Therefore, the train needs to reserve a certain headway time during the entire operation period to ensure safety. The constraint of minimum safe headway can be described as:

$$\begin{aligned} t_{safe} &\le a_{i+1,j} - a_{i,j} \\ t_{safe} &\le d_{i+1,j} - d_{i,j} \end{aligned} \tag{3}$$
$$1 \le i \le K-1, 1 \le j \le J-1$$

(4) Trip Time Constraints: This paper mainly adjusts the dwell time to optimize the timetable without changing the speed curve and running time. At the same time, the arrival time $A_{i,1}$ at the first station and the departure time $D_{i,J}$ at the last station of train i of the original timetable

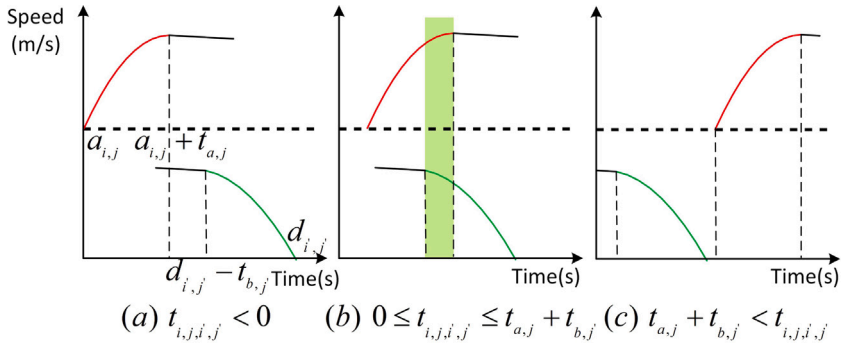

Fig. 1. A sketch of three cases of the overlap time.

must be consistent with the optimized timetable. The trip time of train i from station j to station $j+1$ can be described as:

$$\begin{aligned} & d_{i,j+1} - a_{i,j} = t_{j,j+1} \\ & a_{i,1} = A_{i,1}\ ,\ d_{i,J} = D_{i,J} \\ \forall\ 1 \le i \le K, \quad & 1 \le j \le J-1 \end{aligned} \tag{4}$$

3.2. MILP model

The classic energy-saving driving strategy was adopted in this paper, which utilizes a three-segment type: motoring, coasting, braking (Pudney & Howlett, 1994). Other driving strategies with long periods of traction and braking can also adopt the model in this paper, such as the four-segment type (motoring-cruising-coasting-braking), skipping the coasting mode (motoring-cruising-braking).

Define $t_{i,j,i',j'}$ as the difference between the end time of the maximum accelerating part of train i in interval j and the start time of the maximum braking part of train i' in interval j', which can be described as Eq. (6). As shown in Fig. 1, when $t_{i,j,i',j'} < 0$ or $t_{i,j,i',j'} > t_{a,j} + t_{b,j'}$, it means that there is no overlap time between train i and train i'. At this time, the overlap time is zero. When $0 \le t_{i,j,i',j'} \le t_{a,j} + t_{b,j'}$, there is an overlapping time $t^{ov}_{i,j,i',j'}$ between train i and train i'. The curve of the relationship between $t_{i,j,i',j'}$ and $t^{ov}_{i,j,i',j'}$ in Fig. 2 can be obtained, which can be specifically described as:

$$t^{ov}_{i,j,i',j'} = \begin{cases} 0, & t_{i,j,i',j'} < 0 \\ t_{i,j,i',j'}, & 0 \le t_{i,j,i',j'} \le t^{min}_{i,j,i',j'} \\ t^{min}_{i,j,i',j'}, & t^{min}_{i,j,i',j'} \le t_{i,j,i',j'} \le t^{max}_{i,j,i',j'} \\ \frac{t_{i,j,i',j'} - t_{a,j} - t_{b,j'}}{t^{max}_{i,j,i',j'} - t_{a,j} - t_{b,j'}} \cdot t^{min}_{i,j,i',j'}, & t^{max}_{i,j,i',j'} \le t_{i,j,i',j'} \le t_{a,j} + t_{b,j'} \\ 0, & t_{a,j} + t_{b,j'} < t_{i,j,i',j'} \end{cases} \tag{5}$$

$$t_{i,j,i',j'} = a_{i,j} + t_{a,j} - d_{i',j'} + t_{b,j'} \tag{6}$$

where $t^{max}_{i,j,i',j'}$ is the maximum value of $t_{a,j}$ and $t_{b,j'}$, and $t^{max}_{i,j,i',j'} = max\{t_{a,j}, t_{b,j'}\}$; $t^{min}_{i,j,i',j'}$ is the minimum value of $t_{a,j}$ and $t_{b,j'}$, and $t^{min}_{i,j,i',j'} = min\{t_{a,j}, t_{b,j'}\}$.

When $0 \le t_{i,j,i',j'} \le t_{a,j} + t_{b,j'}$, the logical variable $\alpha_{i,j,i',j'} = 1$ is introduced to determine the overlap time range is $[0, t_{a,j} + t_{b,j'}]$. Logical conditions Eq. (7) and constraints Eq. (8) can be constructed (Floudas, 1995).

$$\begin{aligned} & [\alpha_{i,j,i',j'} = 1] \Rightarrow 0 \le t_{i,j,i',j'} \le t_{a,j} + t_{b,j'} \\ & -M(1 - \alpha_{i,j,i',j'}) \le t_{i,j,i',j'} \le t_{a,j} + t_{b,j'} + M(1 - \alpha_{i,j,i',j'}) \end{aligned} \tag{7}$$

$$s.t. \begin{cases} t^{ov}_{i,j,i',j'} \le t_{i,j,i',j'} + M \cdot (1 - \alpha_{i,j,i',j'}) \\ t^{ov}_{i,j,i',j'} \le t^{min}_{i,j,i',j'} + M \cdot (1 - \alpha_{i,j,i',j'}) \\ t^{ov}_{i,j,i',j'} \le \frac{t_{i,j,i',j'} - t_{a,j} - t_{b,j'}}{t^{max}_{i,j,i',j'} - t_{a,j} - t_{b,j'}} \cdot t^{min}_{i,j,i',j'} + M(1 - \alpha_{i,j,i',j'}) \end{cases} \tag{8}$$

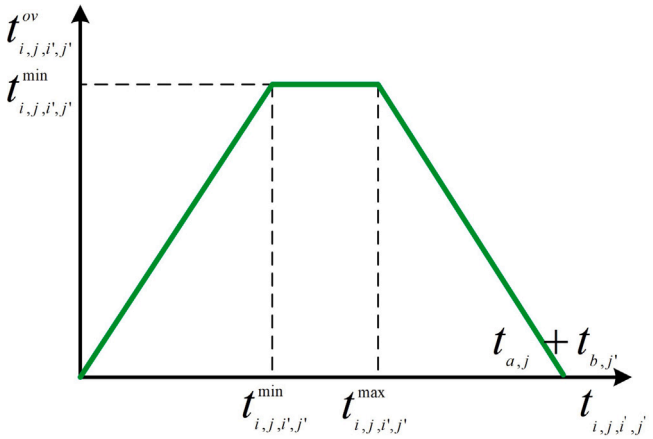

Fig. 2. The curve of the relationship between $t_{i,j,i',j'}$ and $t^{ov}_{i,j,i',j'}$.

When $t_{i,j,i',j'} < 0$ or $t_{i,j,i',j'} > t_{a,j} + t_{b,j'}$, it can be regarded as $t^{ov}_{i,j,i',j'} = 0$. In order to reduce the variables, $\alpha_{i,j,i',j'} = 0$ is utilized to indicate the range of the overlap time, which can be specifically described as:

$$\begin{aligned} & [\alpha_{i,j,i',j'} = 0] \Rightarrow t_{i,j,i',j'} < 0 \quad or \quad t_{a,j} + t_{b,j'} < t_{i,j,i',j'} \\ & t^{ov}_{i,j,i',j'} \le M \cdot \alpha_{i,j,i',j'} \end{aligned} \tag{9}$$

It can be seen from Fig. 2 that $0 \le t^{ov}_{i,j,i',j'} \le t^{min}_{i,j,i',j'}$. Therefore, M can be defined as the maximum value $t^{min}_{i,j,i',j'}$ of the objective function $t^{ov}_{i,j,i',j'}$. The second constraint of Eq. (8) and the constraint of Eq. (9) are repeated. The constraint of Eq. (8) and the constraint of Eq. (7) are repeated.

In practice, the RBE generated in interval j' of train i' maybe be utilized by multiple traction trains simultaneously. The constrained of Eq. (10) is introduced to ensure that the MILP model only counts the highest RBE utilization among all traction trains, which is to improve RBE utilization efficiency.

$$\sum_{i=1}^{I} \sum_{j=1}^{J-1} \alpha_{i,j,i',j'} \le 1, \quad \forall\ 1 \le i' \le K, \quad 1 \le j' \le J-1 \tag{10}$$

Therefore, the number of constraints and variables of the established model is consistent with the number of constraints and variables in the paper (Peña-Alcaraz et al., 2012; Ramos et al., 2008). $\gamma_{j,j'}$ is to judge whether interval j and interval j' belong to the same coordinated optimization interval. Taking the coordination of trains in the same substation interval as an example, when the accelerating train and the braking train are in the same substation interval $\gamma_{j,j'} = 1$, otherwise $\gamma_{j,j'} = 0$. According to Eqs. (1), (2), (3), (4), (6), (8), (9) and (10), the MILP model of the energy-saving timetable optimization can be

described as Eq. (11).

$$Max \quad T = \sum_{i=1}^{I} \sum_{j=1}^{J-1} \sum_{i'=1}^{I} \sum_{j'=1}^{J-1} (\gamma_{j,j'} \cdot t_{i,j,i',j'}^{ov})$$

$$s.t. \begin{cases} t_{i,i+1}^{min} \le d_{i+1,j} - d_{i,j} \le t_{i,i+1}^{max} \\ d_{j,min} \le a_{i,j} - d_{i,j} \le d_{j,max} \\ t_{safe} \le a_{i+1,j} - a_{i,j} \\ t_{safe} \le d_{i+1,j} - d_{i,j} \\ d_{i,j+1} - a_{i,j} = t_{j,j+1} \\ a_{i,1} = A_{i,1}\ ,\ d_{i,J} = D_{i,J} \\ 0 \le t_{i,j,i',j'}^{ov} \le M \cdot \alpha_{i,j,i',j'} \\ t_{i,j,i',j'}^{ov} \le t_{i,j,i',j'} + M \cdot (1 - \alpha_{i,j,i',j'}) \\ t_{i,j,i',j'}^{ov} \le \frac{t_{i,j,i',j'} - t_{a,j} - t_{b,j'}}{t_{i,j,i',j'}^{max} - t_{a,j} - t_{b,j'}} \cdot t_{i,j,i',j'}^{min} + M(1 - \alpha_{i,j,i',j'}) \\ \sum_{i=1}^{I} \sum_{j=1}^{J-1} \alpha_{i,j,i',j'} \le 1, \quad \forall\, i, j, i', j' \end{cases} \tag{11}$$

4. Modeling and solution of DC traction network

Generally, the optimized timetable generated by the overlap time method will not achieve the desired effect in practical applications. The essence of energy utilization is the exchange of power flow, and the overlap time method is a simplification of RBE utilization between trains. Moreover, most of the previous studies on timetable optimization only focused on the transfer and utilization of mechanical energy, and it is difficult to estimate the actual energy transfer and utilization between trains. Therefore, this section will model the DC traction power supply systems, which will provide the basis for the next section to propose a novel timetable optimization method that is more in line with the actual traction power supply systems and to calculate the energy consumption of the simulation.

4.1. Power flow analysis

Some studies have carried out power flow calculations for traction power supply systems (Tian et al., 2014, 2016, 2017). During the power flow analysis, the train can be regarded as an ideal power source. According to the instantaneous train mechanical traction power $P_i(t)$, mechanical braking power $P_i^b(t)$, and auxiliary power $P_i^0(t)$, the actual electrical power of the train can be described as:

$$P_i(t) = P_i^t(t)/\eta - P_i^b(t) \times \eta + P_i^0(t) \tag{12}$$

where η represents electromechanical conversion efficiency.

Coordination scheduling rules are discussed in detail to maximize the utilization of RBE and reduce energy consumption. As shown in Fig. 3, two trains in any substations are accelerating and braking respectively. In the DC traction power supply systems, the line resistance depends on the length and resistivity of the overhead line and the return rail, the traction rectifier substation can be regarded as an ideal voltage source and an equivalent resistance in series (Tian et al., 2016), these values are known in this paper. The power of the train i at time t is $P_i(t)$, the voltage is $U_i(t)$, and the current is $I_i(t)$, where the power is known. Eq. (13) can be utilized as a constraint for power analysis.

$$I_i(t) = \frac{P_i(t)}{U_i(t)} \tag{13}$$

The direction of the train current flowing to the return rail is defined as positive, The direction of the substation current flowing to the overhead line is defined as positive.

The energy of the trains in the bilateral power supply system can also be supplied by the other substations. The DC traction power supply systems cannot be solved by means of simple power flow calculation. According to the nodal method, if the voltages of all nodes and the admittance between each node are known, the current flowing into all nodes can be calculated, which can be specifically described as:

$$[I] = [Y] \times [V] \tag{14}$$

where $[I]$ represents the current matrix flowing into each node; $[Y]$ represents the admittance matrix of the node; $[V]$ represents the voltage matrix of each node to the ground.

4.2. Iterative power flow calculation

According to Eqs. (13) and (14), the voltage and current at each node can be obtained by solving the nonlinear equation systems. According to the obtained node voltage and current of the traction substation at a certain time, the output power of substations at that time can be obtained, and then the energy consumption can be obtained by integrating the output power with time. Therefore, the function of the iterative power flow calculation is to calculate the energy consumption of a certain transient state when considering the traction power supply system.

The nonlinear characteristics of traction substations and trains in the power flow calculation of the traction network make it necessary to approach the actual voltage value through iterative calculation. Therefore, the iterative power flow calculation is utilized to calculate more accurate energy consumption values in the case study.

Algorithm 1 Iterative Power Flow Calculation

Input timetable, train data, line data, set $t = 0$ and initialize the systems states.
repeat
Step 1: Construct the nodal admittance matrix $[Y]$ at time t, go to step 2.
Step 2: Solve for node voltage and current by iteration, go to step 3.
Step 3: If the voltage of the substation is greater than the no-load voltage, go to step 4, otherwise, go to step 8.
Step 4: If substation has been switch off, go to step 5, otherwise, go to step 6.
Step 5: If the voltage of the substation is greater than the overvoltage limitation, go to step 7, otherwise, go to step 8.
Step 6: Switches off the substation, go to step 1.
Step 7: Put into braking resistor, go to step 1.
Step 8: Calculate energy consumption and RBE utilization at time t, set $t = t + 1$.
until The calculation at all times has been completed, that is, $t > t_{max}$.

Output total energy consumption and RBE utilization.

5. The novel optimization method—The overlap current

As shown in Fig. 1, the difference between the acceleration start time of the traction train and the braking start time of the braking train will lead to different utilization of regenerative energy. During the process from case (a) to case (c), the general trend of energy consumption will decrease first then increase, as shown in Fig. 4. This general trend of energy consumption shows the non-linear characteristics of its RBE utilization. Non-linearity usually causes great difficulty in modeling.

As shown in the previous section on the modeling and iterative solution of the DC traction power supply systems, the energy consumption and RBE utilization are difficult to express with explicit equations. Therefore, most of the previous research on timetable optimization only focused on the transfer and utilization of mechanical energy, which did not consider the exchange of energy and the line loss of the actual traction power supply systems. A few papers have carried

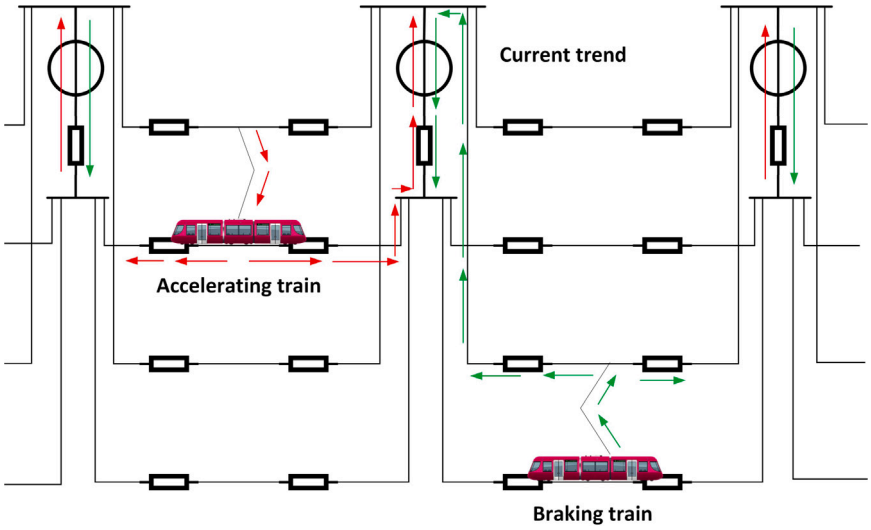

Fig. 3. Traction power supply systems circuit diagram.

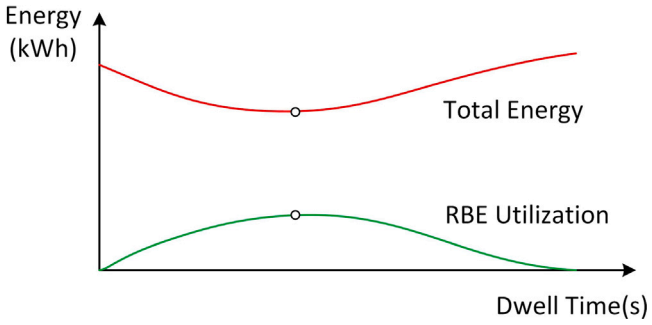

Fig. 4. Trend chart of energy consumption and dwell time.

out research on speed curve optimization or timetable optimization considering traction power supply systems (Pan et al., 2020; Xiao et al., 2020). However, these studies are only applicable to unilateral power supply systems, which also means that the energy transfer and utilization between trains is limited to the same substation. Therefore, this paper proposes an energy transfer and utilization model under the bilateral power supply systems, which can realize the calculation of energy transfer and utilization across different substations.

5.1. The current of the train

The DC traction power supply systems for urban rail transit is a non-linear systems. The voltage $U_i(t)$ across train i at time t is equal to the algebraic sum of the voltage generated across train i when all substations acts as a voltage source and all trains acts as a current source alone, which can be described as:

$$U_i(t) = \sum_{in'=1}^{K} U_{in'}(i,t) + \sum_{in'=I+1}^{K+N} U_{in'}(i,t) \tag{15}$$

When there is no train in the line and only the substation functions, according to the mesh current method and symmetry, it can be known that all tributary currents are zero, and the voltage across the train is U_s. Substituting $\sum_{in'=I+1}^{K+N} U_{in'}(i,t) = Us$ into Eq. (15) can be expressed as:

$$\begin{aligned} U_i(t) &= \sum_{in'=1}^{K} U_{in'}(i,t) + U_s \\ &= U_s + U_i(i,t) + \sum_{in'=1}^{i-1} U_{in'}(i,t) + \sum_{in'=i+1}^{K} U_{in'}(i,t) \end{aligned} \tag{16}$$

The voltage across train i mainly depends on the voltage when all substations acts as a voltage source and train i acts as a current source alone, and $\sum_{in'=1}^{i-1} U_{in'}(i,t) + \sum_{in'=i+1}^{K} U_{in'}(i,t) \ll U_s + U_i(i,t)$. Therefore, Eq. (16) can be simplified to:

$$\begin{aligned} U_i(t) &= U_s + U_i(i,t) \\ &= U_s - I_i(t) \cdot R(x(i,t)) \end{aligned} \tag{17}$$

where $R(x(i,t))$ represents the equivalent resistance of the network at the position $x(i,t)$ of train i.

According to Eqs. (13) and (17), the approximate current of the train i at time t can be obtained as:

$$I_i(t) = \frac{U_s - \sqrt{U_s^2 - 4 \cdot P_i(t) \cdot R(x(i,t))}}{2 \cdot R(x(i,t))} \tag{18}$$

It can be concluded that the current generated at the substation n is $\lambda_i(n,t)$ when the train i at position $x(i,t)$ is utilized as an independent unit current ($I_i(t) = 1$) source through calculation. According to Kirchhoff's current law, the algebraic sum of the current flowing out of a node at any time is zero. It can be derived from this:

$$\sum_{n=1}^{N} \lambda_i(n,t) = 1 \tag{19}$$

According to the homogeneity of the superposition theorem, the current $I_i(n,t)$ generated in the substation n when the current $I_i(t)$ of train i is utilized as an independent current source is:

$$\begin{aligned} I_i(n,t) &= \lambda_i(n,t) \cdot I_i(t) \\ &= \lambda_i(n,t) \cdot \frac{U_s - \sqrt{U_s^2 - 4 \cdot P_i(t) \cdot R(x(i,t))}}{2 \cdot R(x(i,t))} \end{aligned} \tag{20}$$

5.2. The RBE utilization

In the DC traction power systems, the train can be regarded as the current source. According to the superposition theorem of the circuit, the current of any branch is equal to the algebraic sum of the currents generated in the branch when each independent power source acts alone. Therefore, the current $I(n,t)$ of the substation n is equal to the algebraic sum of the current generated in the substation when the equivalent voltage source U_s of the substation n and the equivalent current source $I_i(t)$ of the train i act alone. This can be described as:

$$I(n,t) = \sum_{in'=1}^{K} I_{in'}(n,t) + \sum_{in'=I+1}^{K+N} I_{in'}(n,t) \tag{21}$$

When there is no train in the line and only the substation functions, according to the mesh current method and symmetry, it can be known that all tributary currents are zero. Substituting $\sum_{in'=I+1}^{K+N} I_{in'}(n,t) = 0$ into Eq. (21) can be expressed as:

$$I(n,t) = \sum_{in'=1}^{K} I_{in'}(n,t) \tag{22}$$

When the substation n supplies energy for accelerating trains i at time t, that is, $I(n,t) > 0$, the energy of this substation can be described as:

$$E(n,t) = [Us \cdot I(n,t) - I(n,t)^2 \cdot Rs] \triangle t \tag{23}$$

where $E(n,t)$ is the energy provided by the substation n at time t, and $\triangle t$ is the unit time.

Only when at least one train is accelerating at the same time, can the RBE energy of the braking train be utilized. Most studies believe that the RBE utilization of two coordinated trains can be described as (Li & Lo, 2014; Yang et al., 2014; Yin et al., 2016):

$$E_{i,j,i',j'}(t) = min\{P_{i,j}(t)/\eta, -P_{i',j'}(t) \cdot \eta\} \triangle t \tag{24}$$

where $E_{i,j,i',j'}(t)$ represents the RBE utilization of the braking train; $P_{i,j}(t)$ represents the power of the accelerating train; $P_{i',j'}(t)$ represents the power of the braking train; η represents electromechanical conversion efficiency.

The energy produced by the braking train cannot be directly transmitted to the accelerating train, so Eq. (24) indicates that the RBE utilization is inaccurate. The directions of current generated in the same substation are opposite when the accelerating i train or the braking train i' are utilized as independent current sources. The accelerating train and the braking train are coordinated so that $I_i(n,t)$ and $I_{i'}(n,t)$ can compensate each other, $I(n,t)$ can be reduced. In actual situations, $I(n,t)$ is much smaller than $Us/(2 \cdot Rs)$. For Eq. (23), the energy consumption $E(n,t)$ of the substation will decrease as the current $I(n,t)$ decreases when $I_i(n,t) \le Us/(2 \cdot Rs)$. Therefore, combined with Eqs. (22), (23) and (24), the compensation current generated by the accelerating train and the braking train in the substation can be described as:

$$\begin{aligned} E_{i,j,i',j'}(t) &= \sum_{n=1}^{N} [Us I'(n,t) - I'(n,t)^2 Rs - Us I(n,t) + I(n,t)^2 Rs] \triangle t \\ &= \sum_{n=1}^{N} \{(I'(n,t) - I(n,t))[Us - (I'(n,t) + I(n,t))Rs]\} \triangle t \end{aligned} \tag{25}$$

where $I'(n,t)$ is the current of the substation n before the compensation current generated by the braking train i' appears, and $I(n,t)$ is the compensation current of the substation n after the current generated by the braking train i' appears, that is, $I'(n,t) - I(n,t) = min\{I_i(n,t), -I_{i'}(n,t)\}$. $E_{i,j,i',j'}(t)$ only represents the RBE utilization by compensating the current. Since $(I'(n,t) + I(n,t)) \cdot Rs \ll Us$, in order to facilitate the subsequent construction of the MILP model, Eq. (25) is simplified to:

$$\begin{aligned} E_{i,j,i',j'}(t) = \sum_{n=1}^{N} &[Us \cdot min\{I_i(n,t), -I_{i'}(n,t)\} \\ &- min\{I_i(n,t), -I_{i'}(n,t)\}^2 \cdot Rs] \triangle t \end{aligned} \tag{26}$$

It can be seen from Eq. (26) that the RBE generated by the braking train can be utilized by the accelerating train in any substations. Since $I_i(n,t)$ is the current generated on the substation branch when the voltage source acts alone, for the substation branch on the left or right of the train, the farther away from the train, the smaller the current $I_i(n,t)$. The farther the two coordinated trains are, the smaller the $min\{I_i(n,t), -I_{i'}(n,t)\}$ generated in the same substation, the smaller the RBE utilization $E_{i,j,i',j'}(t)$. Therefore, the utilization of the RBE generated by the braking train to the accelerating train at a long distance is lower than that of the accelerating train at a short distance. Compared with Eqs. (24), (26) expresses the utilization of RBE more accurately, which can realize the utilization of RBE between trains in any intervals, so it can realize the cooperative scheduling of trains in any intervals.

From Eqs. (26) and (20), the RBE utilization $E_{i,j,i',j'}(t)$ can be obtained according to the power and position of the braking train i' and the accelerating train i.

The RBE utilization $E_{i,j,i',j'}$ of the current generated by the accelerating train and the braking train in the substation when the maximum accelerating part of train i at station j overlaps the maximum braking part of train i' at station j' can be expressed as:

$$\begin{aligned} E_{i,j,i',j'} = \sum_{t=1}^{t^{ov}_{i,j,i',j'}} \sum_{n=1}^{N} &[Us \cdot min\{I_i(n,t), -I_{i'}(n,t)\} \\ &- min\{I_i(n,t), -I_{i'}(n,t)\}^2 Rs] \triangle t \end{aligned} \tag{27}$$

where $t^{ov}_{i,j,i',j'}$ represents the overlap time between the maximum acceleration part of train i at station j and the maximum braking part of train i' at station j'; $I_i(n,t)$ and $I_{i'}(n,t)$ can be expressed by Eq. (20).

The objective is to maximize the RBE utilization of all trains which is expressed as:

$$E = \sum_{i=1}^{K} \sum_{j=1}^{J-1} \sum_{i'=1}^{K} \sum_{j'=1}^{J-1} (\gamma_{j,j'} \cdot E_{i,j,i',j'}) \tag{28}$$

where $\gamma_{j,j'}$ is to define whether interval j and interval j' belong to the same coordinated optimization interval. For global optimization, any $\gamma_{j,j'} = 1$.

5.3. MILP model

According to Eq. (27), the utilization of RBE at time $t_{i,j,i',j'}$ can be calculated, and the curve of the relationship between $t_{i,j,i',j'}$ and $E_{i,j,i',j'}$ in Fig. 5(a) can be obtained. The objective function $E_{i,j,i',j'}(t_{i,j,i',j'})$ generated by the accelerating train i in the interval j and the braking train i' in the interval j' shows a trend of increasing first than decreasing.

Piecewise linearization is often utilized to linearize nonlinear functions. Logical variables are often utilized to link segmented functions to achieve linearization (Floudas, 1995). The segmented objective function can be represented by introducing logical variables. The objective function $E_{i,j,i',j'}$ of Fig. 5(a) is divided into the four intervals shown in Fig. 5(b) to achieve the same scale as the previous overlap time method, which can be specifically described as:

$$E_{i,j,i',j'} = \begin{cases} 0, & t_{i,j,i',j'} < 0 \\ \frac{E^m_{i,j,i',j'}}{t^m_{i,j,i',j'}} \cdot t_{i,j,i',j'}, & 0 \le t_{i,j,i',j'} \le t^m_{i,j,i',j'} \\ \frac{t_{i,j,i',j'} - t_{a,j} - t_{b,j'}}{t^m_{i,j,i',j'} - t_{a,j} - t_{b,j'}} \cdot E^m_{i,j,i',j'}, & t^m_{i,j,i',j'} \le t_{i,j,i',j'} \le t_{a,j} + t_{b,j'} \\ 0, & t_{i,j,i',j'} > t_{a,j} + t_{b,j'} \end{cases} \tag{29}$$

where $E^m_{i,j,i',j'}$ is the maximum value of the RBE utilization $E_{i,j,i',j'}$, and $E^m_{i,j,i',j'} = E_{i,j,i',j'}(t^m_{i,j,i',j'})$.

Fig. 6 compares the relationship between the overlap time $t^{ov}_{i,j,i',j'}$ in the overlap time method and the overlap energy $E_{i,j,i',j'}$ in the overlap current method. For the overlap time method, the overlap time of the optimized curves will be more concentrated in $[t^{min}_{i,j,i',j'}, t^{max}_{i,j,i',j'}]$, and there will be multiple optimal solutions. The overlap current method will make the overlap time more concentrated at the time $t^m_{i,j,i',j'}$, which can obtain the optimal solution with the maximum RBE utilization.

When $0 \le t_{i,j,i',j'} \le t_{a,j} + t_{b,j'}$, the logical variable $\alpha_{i,j,i',j'} = 1$ is introduced to determine the overlap time range is $[0, t_{a,j} + t_{b,j'}]$. Logical conditions Eq. (30) and constraints Eq. (31) can be constructed.

$$\begin{aligned} &[\alpha_{i,j,i',j'} = 1] \Rightarrow 0 \le t_{i,j,i',j'} \le t_{a,j} + t_{b,j'} \\ &-M(1 - \alpha_{i,j,i',j'}) \le t_{i,j,i',j'} \le t_{a,j} + t_{b,j'} + M(1 - \alpha_{i,j,i',j'}) \end{aligned} \tag{30}$$

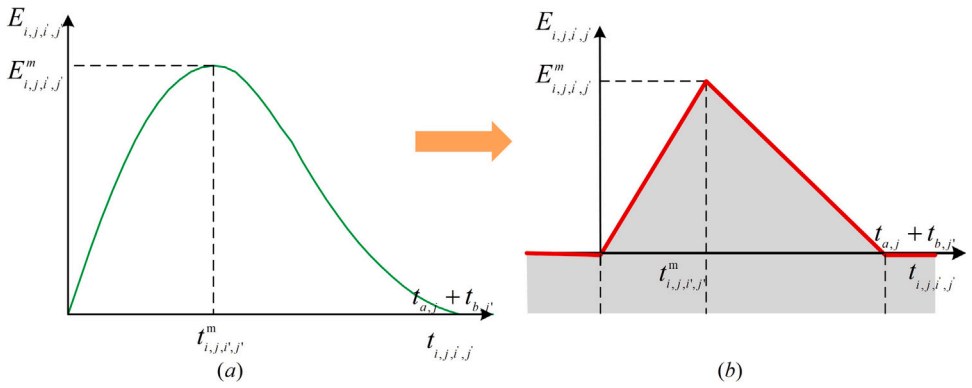

Fig. 5. The curve of the relationship between $t_{i,j,i',j'}$ and $E_{i,j,i',j'}$.

$$s.t.\begin{cases} E_{i,j,i',j'} \le \frac{E^m_{i,j,i',j'}}{t^m_{i,j,i',j'}} \cdot t_{i,j,i',j'} + M(1-\alpha_{i,j,i',j'}) \\ E_{i,j,i',j'} \le \frac{t_{i,j,i',j'}-t_{a,j}-t_{b,j'}}{t^m_{i,j,i',j'}-t_{a,j}-t_{b,j'}} E^m_{i,j,i',j'} + M(1-\alpha_{i,j,i',j'}) \end{cases} \tag{31}$$

It can be seen from Fig. 5 that $0 \le E_{i,j,i',j'} \le E^m_{i,j,i',j'}$. Therefore, M can be defined as the maximum value $E^m_{i,j,i',j'}$ of the objective function $E_{i,j,i',j'}$. The constraint of Eq. (31) and the constraint of Eq. (30) are repeated.

When $t_{i,j,i',j'<0}$ or $t_{i,j,i',j'} > t_{a,j}+t_{b,j'}$, it can be regarded as $E_{i,j,i',j'} = 0$. In order to reduce the variables, $\alpha_{i,j,i',j'} = 0$ is introduced to indicate the range of the overlap time, which can be specifically described as:

$$\begin{aligned} &[\alpha_{i,j,i',j'} = 0] \Rightarrow t_{i,j,i',j'} < 0 \quad or \quad t_{a,j}+t_{b,j'} < t_{i,j,i',j'} \\ &E_{i,j,i',j'} \le M \cdot \alpha_{i,j,i',j'} \end{aligned} \tag{32}$$

According to Eqs. (1), (2), (3), (4), (6), (10), (28), (31), and (32), the MILP model of the energy-saving timetable optimization can be described as Eq. (33). This paper utilizes the Gurobi solver to solve the MILP model.

$$Max \quad E = \sum_{i=1}^{I}\sum_{j=1}^{J-1}\sum_{i'=1}^{I}\sum_{j'=1}^{J-1}(\gamma_{j,j'} \cdot E_{i,j,i',j'})$$

$$s.t.\begin{cases} t^{min}_{i,i+1} \le d_{i+1,j} - d_{i,j} \le t^{max}_{i,i+1} \\ d_{j,min} \le a_{i,j} - d_{i,j} \le d_{j,max} \\ t_{safe} \le a_{i+1,j} - a_{i,j} \\ t_{safe} \le d_{i+1,j} - d_{i,j} \\ d_{i,j+1} - a_{i,j} = t_{j,j+1} \\ a_{i,1} = A_{i,1}\ ,\ d_{i,J} = D_{i,J} \\ 0 \le E_{i,j,i',j'} \le M \cdot \alpha_{i,j,i',j'} \\ E_{i,j,i',j'} \le \frac{E^m_{i,j,i',j'}}{t^m_{i,j,i',j'}} \cdot t_{i,j,i',j'} + M(1-\alpha_{i,j,i',j'}) \\ E_{i,j,i',j'} \le \frac{t_{i,j,i',j'}-t_{a,j}-t_{b,j'}}{t^m_{i,j,i',j'}-t_{a,j}-t_{b,j'}} E^m_{i,j,i',j'} + M(1-\alpha_{i,j,i',j'}) \\ \sum_{i=1}^{I}\sum_{j=1}^{J-1}\alpha_{i,j,i',j'} \le 1, \quad \forall\, i,j,i',j' \end{cases} \tag{33}$$

6. Case study

Many groups of comparative experiments were carried out based on the data of the Beijing Batong Line to verify the effectiveness of the above model in terms of energy saving. As shown in Fig. 7, the Beijing Batong Line consists of 14 stations and 12 substations. The train marshaling method is 3M3T, which the number of vehicles N is 6. A total of 20 trains in the bilateral direction were utilized for experimental comparison. The EMU has a mass M of 288.08t, the coefficient of rotating mass is 0.08, the electromechanical conversion efficiency is 0.85, and the auxiliary power is 45 kW. The required traction energy consumption of the train is 4326.14 kWh, and the

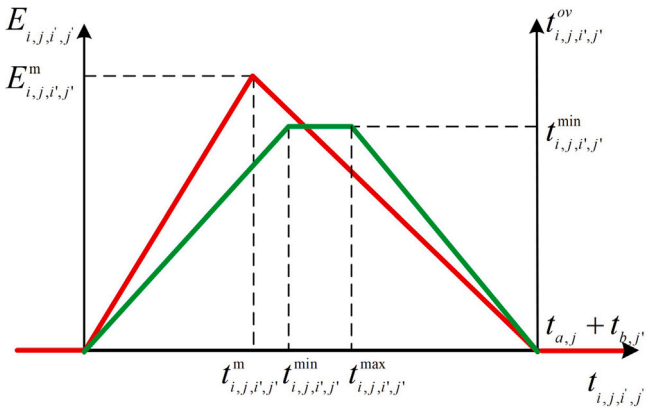

Fig. 6. The curve of the relationship between $t^{ov}_{i,j,i',j'}$ and $E_{i,j,i',j'}$.

Table 1
The DC traction power supply systems parameters of Beijing Batong Line.

Parameters	Value	Unit
Overvoltage limitation	900	V
Substation no-load voltage	825	V
Substation rated voltage	750	V
Auxiliary power	100	kW
Substation inner resistance	0.02	Ω
Traction network unit resistance	0.0081	Ω/km
Rail unit resistance	0.0136	Ω/km

generated RBE of the train is 1772.20 kWh. The average absolute error when linearized from Fig. 5(a) to (b) is only 0.259 kWh. The maximum traction force $F_{max}(v)$ (kN), maximum braking force $B_{max}(v)$ (kN), and basic resistance $W_0(v)$ (kN) can be described as:

$$F_{max}(v) = \begin{cases} 263.9 & 0 \le v \le 43 \\ 263.9 \cdot 43/v & 43 < v \le 50 \\ 263.9 \cdot 43 \cdot 50/v^2 & 50 < v \le 80 \end{cases}$$

$$B_{max}(v) = \begin{cases} 224.9 & 0 \le v \le 75 \\ 224.9 \cdot 75 \cdot 75/v^2 & 75 < v \le 90 \end{cases} \tag{34}$$

$$W_0(v) = 4.94 + 0.04v + 0.0008v^2$$

Many previous studies lacked the modeling of DC traction power supply systems. The influence of the traction power supply systems on the optimization efficiency of the model is obvious. The DC traction power supply systems parameters of Beijing Batong Line are shown in Table 1.

The departure interval of the original timetable is 180 s, and the constraint range $[d_{j,min}, d_{j,max}]$ of the departure interval of adjacent

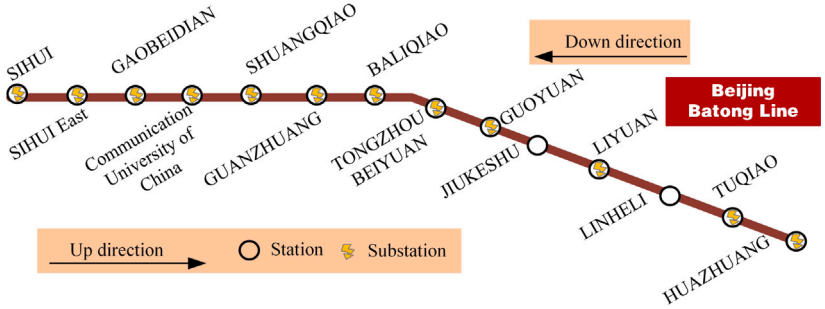

Fig. 7. Line data of stations and substations on Beijing Batong Line.

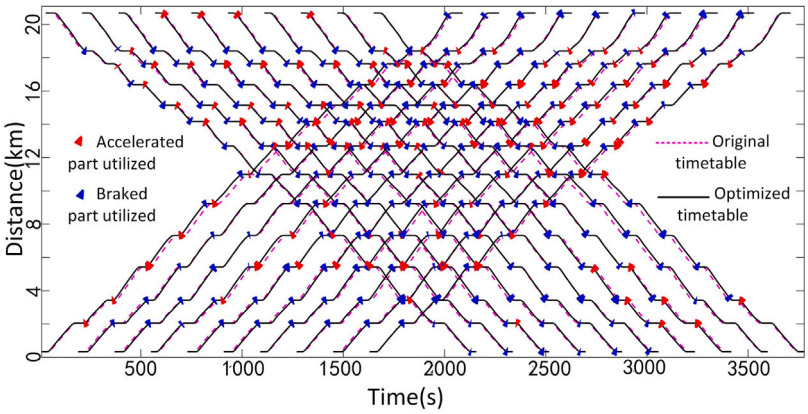

Fig. 8. Optimized timetable by coordinating the trains of all substation and utilizing the overlap current method.

trains is 160–200 s. The minimal safe headway t_{safe} of adjacent trains is 20 s. Table 2 shows the running time (s) and dwell time (s) parameters of the original timetable and the optimized timetable in the bilateral direction.

This paper compared the overlap time method with previous studies and the overlap current method in this paper by coordinating trains in the same substation and all substations to verify the energy-efficient of different methods. At the same time, the DC traction power supply systems calculation is utilized to calculate the energy consumption and RBE utilization. The energy consumption calculation method utilized in most previous studies is the superposition of traction and braking energy in the same substation, but this method does not consider the influence of the traction power supply system. Therefore, this paper also adopts two different methods to calculate energy consumption and RBE utilization, namely, the energy superposition method and the iterative power flow calculation method considering the traction power supply system. The optimized timetable is shown in Fig. 8. Table 3 compares the results of the different optimization methods.

The first group of experiments coordinated the trains to maximize the overlap time. The RBE utilization of trains in the same substation is higher than that of trains in distant power supply sections, so some studies often coordinate trains in the same substation to maximize the RBE utilization. When using the energy superposition method to calculate energy consumption, it is found that the energy-saving rate of coordinated trains in the same substation has increased by 3.78% and the energy-saving rate of coordinated trains in all substations has even decreased by 2.36%. This is because the transfer and utilization of energy between trains across different substations will not be counted. Therefore, the overlap time method is not suitable for timetable optimization of coordinated trains in all substations. However, when the iterative power flow calculation considering the traction power supply system is utilized, the actual energy-saving rate of coordinated trains in the same substation decreases from 3.78% to 0.18%. On the contrary, the actual energy-saving rate of coordinating trains in all substations is as high as 2.39%, which is generally considered to be inefficient. At the same time, the RBE utilization calculated by the energy superposition method is generally low, the actual RBE utilization of coordinated trains in the same substation increases from 11.74% to 58.64%. The reason for this is that the RBE generated by the braking train can be utilized not only by the traction train in the same substation but also by other traction trains in different substations.

Table 2
Original timetable and optimized timetable parameters.

Interval	Running time		Original dwell time		Optimized dwell time	
	Up	Down	Up	Down	Up	Down
SIH	140	140	30	30	25–40	25–40
SIH East	120	120	45	45	40–55	40–55
GAO	140	140	25	30	20–35	25–40
CUC	140	140	30	30	25–40	25–40
SHU	140	140	30	30	25–40	25–40
GUA	150	150	30	30	25–40	25–40
BAL	140	140	30	40	25–40	35–50
TON	120	120	30	30	25–40	25–40
GUO	90	90	30	40	25–40	35–50
JIU	110	110	30	50	25–40	45–60
LIY	100	100	30	50	25–40	45–60
LIN	85	80	30	30	25–40	25–40
TUQ	160	160	30	30	25–40	25–40
HUA	160	160	45	40	40–55	27–42

The second group of experiments coordinated the trains to maximize the overlap current. This is a very novel timetable optimization method that fully considers the characteristics of the traction power supply system. Regardless of the energy calculation method utilized, the timetable optimized by the overlap current method is more energy efficient than the overlap time method. Likewise, the actual energy-saving rate of coordinated trains in the same substation decreases from 4.53% to 1.46%. Although the energy-saving rate of the overlap

Table 3
Comparison of the results of the optimization methods when the departure interval is 180 s.

Calculation method	Index	Original	Overlap time		Overlap current	
			Same substation	All substations	Same substation	All substations
Energy superposition	Utilization of RBE\%	5.87	11.74	3.89	14.05	6.37
	Total energy consumption\kWh	3746.60	3604.87	3834.90	3576.83	3766.15
	Rate of energy saving\%	–	3.78	−2.36	4.53	−0.52
Iterative power flow calculation	Utilization of RBE\%	58.19	58.64	62.66	60.73	68.46
	Total energy consumption\kWh	3413.23	3407.19	3331.68	3363.43	3221.78
	Rate of energy saving\%	–	0.18	2.39	1.46	5.61

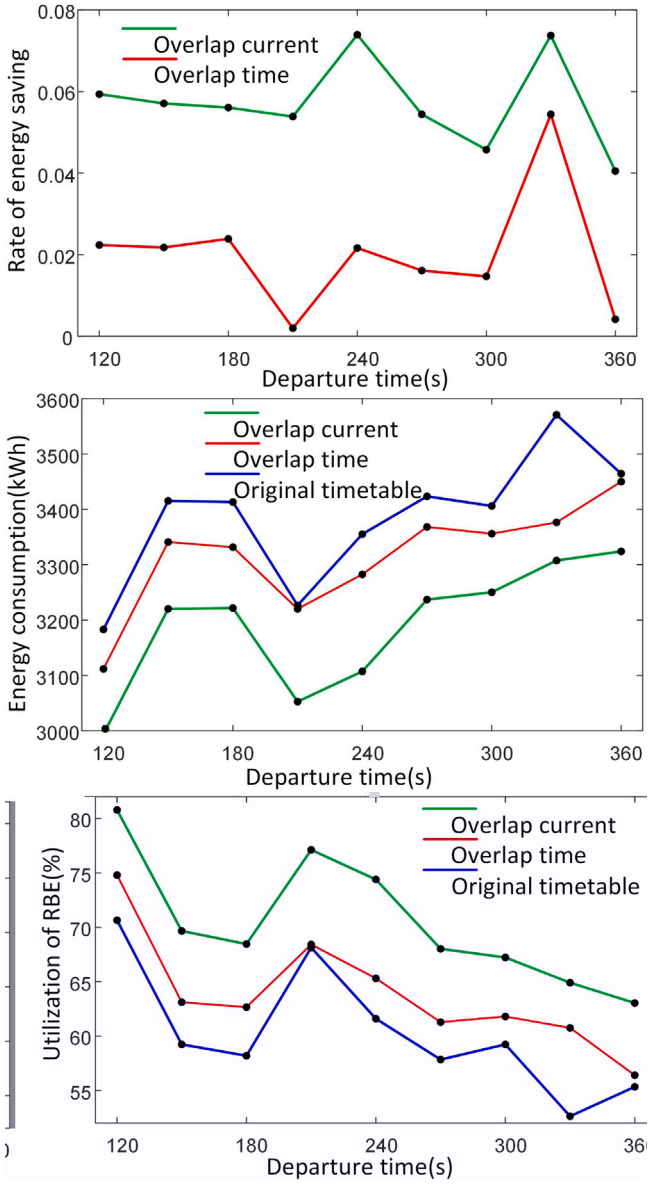

Fig. 9. The impact of different departure intervals on the optimized results.

currents of coordinating trains in the same substation increases from 0.18% to 1.46%, the energy efficient is limited for the interconnected bilateral traction power supply system. The overlap current method proposed in this paper is suitable for coordinating trains in different substations. Compared with the original timetable, the RBE utilization of the overlap currents of coordinating trains in all substations has increased by 10.27%, and the energy-saving rate has increased by 5.61%. The energy-saving effect of the overlap current method has been effectively verified. The reason why the overlap current method is more energy-saving is that it can more accurately represent the utilization of RBE.

It can be seen from Table 3 that coordinating trains in any substations to achieve energy-saving has a significant energy-saving effect. The difference in departure interval of adjacent trains often has a greater impact on the optimization results, so the departure interval of the original timetable is adjusted to 120–360 s. So Fig. 9 compares the impact of different departure intervals on the optimized results of coordinating trains in any substations. The energy-saving effect of the overlap current method is the best when the departure interval is 240 s. The highest energy-saving rate of the overlap current method is 7.39%, and the highest RBE utilization is increased by 12.8%. Compared with the overlap time method, the overlap current method can achieve significant energy-saving under different departure intervals. The overlap current can still ensure a stable energy-saving effect when the departure interval is long, which shows that the overlap current method is more feasible and reproducible.

7. Conclusion

The most fundamental solution to achieving energy-saving is to reduce the energy supply of substations. Therefore, this paper constructs a cross-substation energy transmission and utilization model of the bilateral power supply system according to the energy supply change of the actual traction substation. An overlap current method is proposed to reduce the total energy consumption of the traction substation of the urban rail transit systems by adjusting the dwell time. This method achieves energy-saving by maximizing compensation for the current generated by the accelerating and braking trains in any substations, which takes into account the line loss of the traction power supply systems. This paper linearizes the nonlinear traction power supply system and constructs the MILP model to maximize the utilization of RBE. The iterative power flow calculation method presents entirely different results from the energy superposition method, which obtains a more precise energy utilization and a more realistic RBE utilization. The multi-group simulation results show that the overlap current method proposed in this paper has a significant energy-efficient compared with the overlap time method, the highest RBE utilization was increased by 12.8%, and the highest energy-saving rate was increased by 7.39%.

Although the overlap current method proposed in this paper can greatly reduce the total power supply of the traction substation, the impact of passenger flow and disturbance is worthy of further research.

CRediT authorship contribution statement

Pengfei Sun: Writing – original draft, Writing – review & editing, Methodology, Software. **Chuanxin Zhang:** Writing – original draft, Writing – review & editing, Methodology, Software. **Bo Jin:** Conceptualization, Supervision. **Qingyuan Wang:** Visualization, Supervision. **Haoran Geng:** Visualization, Formal analysis, Conceptualization.

Data availability

No data was used for the research described in the article.

Acknowledgments

This work was supported by the National Natural Science Foundation of China (Nos. U1934221, 62003283).

References

Amit, I., & Goldfarb, D. (1971). The timetable problem for railways. *Developments in Operations Research*, *2*(1), 379–387.

Bai, Y., Cao, Y., Yu, Z., Ho, T. K., Roberts, C., & Mao, B. (2019). Cooperative control of metro trains to minimize net energy consumption. *IEEE Transactions on Intelligent Transportation Systems*, *21*(5), 2063–2077.

Campillo, J., Ghaviha, N., Zimmerman, N., & Dahlquist, E. (2015). Flow batteries use potential in heavy vehicles. In *2015 International conference on electrical systems for aircraft, railway, ship propulsion and road vehicles* (pp. 1–6). IEEE.

Chen, M., Xiao, Z., Sun, P., Wang, Q., Jin, B., & Feng, X. (2019). Energy-efficient driving strategies for multi-train by optimization and update speed profiles considering transmission losses of regenerative energy. *Energies*, *12*(18), 3573.

Chen, X., Zuo, T., Lang, M., Li, S., & Li, S. (2022). Integrated optimization of transfer station selection and train timetables for road–rail intermodal transport network. *Computers & Industrial Engineering*, *165*, Article 107929.

Cordone, R., & Redaelli, F. (2011). Optimizing the demand captured by a railway system with a regular timetable. *Transportation Research, Part B (Methodological)*, *45*(2), 430–446.

D'Ariano, A., Pranzo, M., & Hansen, I. A. (2007). Conflict resolution and train speed coordination for solving real-time timetable perturbations. *IEEE Transactions on intelligent transportation systems*, *8*(2), 208–222.

Du, G., Zhu, C., Jiang, X., Li, Q., Huang, W., Shi, J., et al. (2022). Multi-objective optimization of traction substation converter characteristic and train timetable in subway systems. *IEEE Transactions on Transportation Electrification*.

Floudas, C. A. (1995). *Nonlinear and mixed-integer optimization: Fundamentals and applications*. Oxford University Press.

Gao, Z., Fang, J., Zhang, Y., Jiang, L., Sun, D., & Guo, W. (2015). Control of urban rail transit equipped with ground-based supercapacitor for energy saving and reduction of power peak demand. *International Journal of Electrical Power & Energy Systems*, *67*, 439–447.

González-Gil, A., Palacin, R., & Batty, P. (2013). Sustainable urban rail systems: Strategies and technologies for optimal management of regenerative braking energy. *Energy conversion and management*, *75*, 374–388.

Gupta, S. D., Tobin, J. K., & Pavel, L. (2016). A two-step linear programming model for energy-efficient timetables in metro railway networks. *Transportation Research, Part B (Methodological)*, *93*, 57–74.

Hong, X., Meng, L., D'Ariano, A., Veelenturf, L. P., Long, S., & Corman, F. (2021). Integrated optimization of capacitated train rescheduling and passenger reassignment under disruptions. *Transportation Research Part C (Emerging Technologies)*, *125*, Article 103025.

Huang, Y., Yang, L., Tang, T., Cao, F., & Gao, Z. (2016). Saving energy and improving service quality: Bicriteria train scheduling in urban rail transit systems. *IEEE Transactions on Intelligent Transportation Systems*, *17*(12), 3364–3379.

Jin, B., Feng, X., Wang, Q., & Sun, P. (2022). Real-time train regulation method for metro lines with substation peak power reduction. *Computers & Industrial Engineering*, *168*, Article 108113.

Jin, B., Feng, X., Wang, Q., Sun, P., & Fang, Q. (2021). Train scheduling method to reduce substation energy consumption and peak power of metro transit systems. *Transportation Research Record*, Article 0361198120974677.

Kim, K., Kim, K., & Han, M. (2011). A model and approaches for synchronized energy saving in timetabling. *Korea Railroad Research Institute*.

Lesel, J., Bourdon, D., Claisse, G., Debay, P., & Robyns, B. (2017). Real time electrical power estimation for the energy management of automatic metro lines. *Mathematics and Computers in Simulation*, *131*, 3–20.

Li, X., & Lo, H. K. (2014). An energy-efficient scheduling and speed control approach for metro rail operations. *Transportation Research, Part B (Methodological)*, *64*, 73–89.

Liao, J., Zhang, F., Zhang, S., Yang, G., & Gong, C. (2021). Energy-saving optimization strategy of multi-train metro timetable based on dual decision variables: A case study of shanghai metro line one. *Journal of Rail Transport Planning & Management*, *17*, Article 100234.

Lin, B., & Xie, C. (2014). Energy substitution effect on transport industry of China-based on trans-log production function. *Energy*, *67*, 213–222.

Lindner, T. (2003). *Train schedule optimization in public rail transport*. Mathematics — Key Technology for the Future.

Liu, P., Schmidt, M., Kong, Q., Wagenaar, J. C., Yang, L., Gao, Z., et al. (2020). A robust and energy-efficient train timetable for the subway system. *Transportation Research Part C (Emerging Technologies)*, *121*, Article 102822.

Liu, P., Yang, L., Gao, Z., Huang, Y., Li, S., & Gao, Y. (2018). Energy-efficient train timetable optimization in the subway system with energy storage devices. *IEEE Transactions on Intelligent Transportation Systems*, *19*(12), 3947–3963.

Liu, H., Zhou, M., Guo, X., Zhang, Z., Ning, B., & Tang, T. (2018). Timetable optimization for regenerative energy utilization in subway systems. *IEEE Transactions on Intelligent Transportation Systems*, *20*(9), 3247–3257.

Liu, D., Zhu, S.-Q., Bi, Y.-R., Liu, K., & Xu, Y.-X. (2020). Research on the utilization of metro regenerative braking energy based on an improved differential evolution algorithm. *Journal of Advanced Transportation*, *2020*.

Meng, X., Jia, L., & Qin, Y. (2010). Train timetable optimizing and rescheduling based on improved particle swarm algorithm. *Transportation Research Record*, *2197*(1), 71–79.

Meng, L., & Zhou, X. (2011). Robust single-track train dispatching model under a dynamic and stochastic environment: A scenario-based rolling horizon solution approach. *Transportation Research, Part B (Methodological)*, *45*(7), 1080–1102.

Nasri, A., Moghadam, M. F., & Mokhtari, H. (2010). Timetable optimization for maximum usage of regenerative energy of braking in electrical railway systems. In *SPEEDAM 2010* (pp. 1218–1221).

Ning, J., Zhou, Y., Long, F., & Tao, X. (2018). A synergistic energy-efficient planning approach for urban rail transit operations. *Energy*, *151*, 854–863.

Pan, Z., Chen, M., Lu, S., Tian, Z., & Liu, Y. (2020). Integrated timetable optimization for minimum total energy consumption of an AC railway system. *IEEE Transactions on Vehicular Technology*, *69*(4), 3641–3653.

Peña-Alcaraz, M., Fernández, A., Cucala, A. P., Ramos, A., & Pecharromán, R. R. (2012). Optimal underground timetable design based on power flow for maximizing the use of regenerative-braking energy. *Proceedings of the Institution of Mechanical Engineers, Part F: Journal of Rail and Rapid Transit*, *226*(4), 397–408.

Pudney, P., & Howlett, P. (1994). Optimal driving strategies for a train journey with speed limits. *The ANZIAM Journal*, *36*(1), 38–49.

Pugi, L., Grasso, F., & Rossi, G. (2018). Energy simulation of tramway systems, simplified and efficient models. In *2018 IEEE international conference on environment and electrical engineering and 2018 IEEE industrial and commercial power systems Europe (EEEIC/I&CPS Europe)* (pp. 1–6). IEEE.

Ramos, A., Pena, M. T., Fernández, A., & Cucala, P. (2008). Mathematical programming approach to underground timetabling problem for maximizing time synchronization. *Dirección y Organización*, (35), 88–95.

Rupp, A., Baier, H., Mertiny, P., & Secanell, M. (2016). Analysis of a flywheel energy storage system for light rail transit. *Energy*, *107*, 625–638.

Shao, J., Xu, Y., Sun, L., Kong, D., & Lu, H. (2022). Equity-oriented integrated optimization of train timetable and stop plans for suburban railways system. *Computers & Industrial Engineering*, Article 108721.

Su, S., Wang, X., Cao, Y., & Yin, J. (2019). An energy-efficient train operation approach by integrating the metro timetabling and eco-driving. *IEEE Transactions on Intelligent Transportation Systems*, *21*(10), 4252–4268.

Tang, H., Dick, C. T., & Feng, X. (2015). Improving regenerative energy receptivity in metro transit systems: Coordinated train control algorithm. *Transportation Research Record*, *2534*(1), 48–56.

Tian, Z., Hillmansen, S., Roberts, C., Weston, P., Chen, L., Zhao, N., et al. (2014). Modeling and simulation of DC rail traction systems for energy saving. In *17th International IEEE conference on intelligent transportation systems* (pp. 2354–2359). IEEE.

Tian, Z., Hillmansen, S., Roberts, C., Weston, P., Zhao, N., Chen, L., et al. (2016). Energy evaluation of the power network of a DC railway system with regenerating trains. *IET Electrical Systems in Transportation*, *6*(2), 41–49.

Tian, Z., Weston, P., Zhao, N., Hillmansen, S., Roberts, C., & Chen, L. (2017). System energy optimisation strategies for metros with regeneration. *Transportation Research Part C (Emerging Technologies)*, *75*, 120–135.

Xiao, Z., Feng, X., Wang, Q., & Sun, P. (2020). Eco-driving control for hybrid electric trams on a signalised route. *IET Intelligent Transport Systems*, *14*(1), 36–44.

Xie, J., Zhang, J., Sun, K., Ni, S., & Chen, D. (2021). Passenger and energy-saving oriented train timetable and stop plan synchronization optimization model. *Transportation Research Part D: Transport and Environment*, *98*, Article 102975.

Xun, J., Liu, T., Ning, B., & Liu, Y. (2019). Using approximate dynamic programming to maximize regenerative energy utilization for metro. *IEEE Transactions on Intelligent Transportation Systems*, *21*(9), 3650–3662.

Yang, X., Chen, A., Li, X., Ning, B., & Tang, T. (2015). An energy-efficient scheduling approach to improve the utilization of regenerative energy for metro systems. *Transportation Research Part C (Emerging Technologies)*, *57*, 13–29.

Yang, X., Li, X., Gao, Z., Wang, H., & Tang, T. (2012). A cooperative scheduling model for timetable optimization in subway systems. *IEEE Transactions on Intelligent Transportation Systems*, *14*(1), 438–447.

Yang, X., Ning, B., Li, X., & Tang, T. (2014). A two-objective timetable optimization model in subway systems. *IEEE Transactions on Intelligent Transportation Systems*, *15*(5), 1913–1921.

Yang, X., Wu, J., Sun, H., Gao, Z., Yin, H., & Qu, Y. (2019). Performance improvement of energy consumption, passenger time and robustness in metro systems: A multi-objective timetable optimization approach. *Computers & Industrial Engineering*, *137*, Article 106076.

Yin, J., Tang, T., Yang, L., Gao, Z., & Ran, B. (2016). Energy-efficient metro train rescheduling with uncertain time-variant passenger demands: An approximate dynamic programming approach. *Transportation Research, Part B (Methodological)*, *91*, 178–210.

Zhang, H., Li, S., & Yang, L. (2019). Real-time optimal train regulation design for metro lines with energy-saving. *Computers & Industrial Engineering*, *127*, 1282–1296.

Zhao, N., Roberts, C., Hillmansen, S., Tian, Z., Weston, P., & Chen, L. (2017). An integrated metro operation optimization to minimize energy consumption. *Transportation Research Part C (Emerging Technologies)*, *75*, 168–182.

Zhong, Z., Yang, Z., Fang, X., Lin, F., & Tian, Z. (2020). Hierarchical optimization of an on-board supercapacitor energy storage system considering train electric braking characteristics and system loss. *IEEE Transactions on Vehicular Technology*, *69*(3), 2576–2587.